Fitoterapia 135 (2019) 99–106

Contents lists available at ScienceDirect

Fitoterapia

journal homepage: www.elsevier.com/locate/fitote

Absolute structure assignment of an iridoid-monoterpenoid indole alkaloid hybrid from *Dipsacus asper*

Zhi-Pu Yu[a,b], Yin-Yin Wang[b], Shu-Juan Yu[a,b], Jie Bao[b], Jin-Hai Yu[b,*], Hua Zhang[b,*]

[a] School of Chemistry and Chemical Engineering, University of Jinan, 336 West Road of Nan Xinzhuang, Jinan 250022, China
[b] School of Biological Science and Technology, University of Jinan, 336 West Road of Nan Xinzhuang, Jinan 250022, China

ARTICLE INFO

Keywords:
Dipsacus asper
Glucoindole alkaloid
Iridoid glucoside
Cytotoxicity
Calculated ECD
AChE inhibition

ABSTRACT

Iridoid-monoterpenoid indole alkaloid hybrids (IMIAHs) represent a rare class of natural products reported from only several plants of Rubiaceae and Dipsacaceae families, while their structural assignments remain a very challenging work due to complexity and flexibility. In the current study, a new IMIAH (**1**) was isolated from the roots of *Dipsacus asper* and its structure with absolute configuration was unambiguously established by a combination of spectroscopic analyses, chemical degradation and ECD calculation. A new oleanane-type triterpenoid saponin (**2**) and 15 known co-metabolites were also obtained and structurally characterized. Our biological evaluations showed that compound **2** exhibited moderate inhibition against acetylcholine esterase (AChE) with an IC_{50} value of 15.8 ± 0.56 μM, and compound **15** displayed potent cytotoxicity selectively against human A549 and H157 lung cancer cells with IC_{50} values of 6.94 ± 0.24 and 9.06 ± 0.12 μM, respectively.

1. Introduction

Indole alkaloids with a non-rearranged iridoid unit, *e.g.* strictosidine, are key biosynthetic intermediates of the commonly known monoterpenoid (rearranged) indole alkaloids (MIAs) [1] which have afforded several famous anticancer drugs such as vinblastine and vincristine. As the number of non-rearranged MIAs increases in the literature, a few hybrids of them with an extra iridoid moiety have also been reported [2–5]. Biogenetically, these iridoid-monoterpenoid indole alkaloid hybrids (IMIAHs) originate from the condensation of a trypotamine/tryptophan with two iridoid glucosides, and so far they have only been obtained from several plants of Rubiaceae and Dipsacaceae families [2–5]. The core structure of a typical IMIAH is as shown in 5*S*-5-carboxyvincoside and 5*S*-5-carboxystrictosidine (Fig. 1), and C-3, *N*-4, C-6 and C-22 are the general connecting sites of the second iridoid unit. These molecules present tremendous flexibilities which have brought great challenge to their structural elucidation especially for the assignment of absolute configuration.

Following our earlier investigation into the EtOAc partition of the ethanol extract from *D. asper* [6], the current study on the polar *n*-BuOH partition afforded an new IMIAH (**1**) incorporating a 22-*O*-iridoid glucoside unit *via* an ester bond. The planar structure of **1** was first established *via* spectroscopic analyses, and the absolute configuration was further determined by a series of chemical methods and theoretical computations. To the best of our knowledge, it is only the second report of IMIAH with a C-22 linkage. In addition, a new oleanane-type triterpenoid saponin (**2**) and 15 known compounds were also isolated and identified.

The *in vitro* cytotoxicity of all the isolates were evaluated against four human cancer cell lines, A549 (lung), H157 (lung), HepG2 (liver) and MCF-7 (breast), and compound **15** exhibited selective inhibitory activity against the two lung cancer cells. Moreover, the acetylcholine esterase (AChE) inhibitory assay established that compound **2** was a moderate AChE inhibitor. Herein, the isolation, structural elucidation and biological evaluations of these natural products are described below.

2. Experimental section

2.1. General experimental procedures

Optical rotations were measured on a Rudolph VI polarimeter (Rudolph Research Analytical, Hackettstown, USA) with a 10 cm length cell. UV and CD spectra were obtained on a Chirascan Spectrophotometer (Applied Photophysics Ltd., Leatherhead, UK) with a 0.1 cm pathway cell. IR spectra were recorded on a VERTEX70 spectrometer (Bruker Optics Inc., Billerica, USA) with KBr disks. NMR experiments were performed on a Bruker Avance DRX600 spectrometer

* Corresponding authors.
E-mail addresses: bio_yujh@ujn.edu.cn (J.-H. Yu), bio_zhangh@ujn.edu.cn (H. Zhang).

https://doi.org/10.1016/j.fitote.2019.04.015
Received 2 April 2019; Received in revised form 26 April 2019; Accepted 27 April 2019
Available online 30 April 2019
0367-326X/

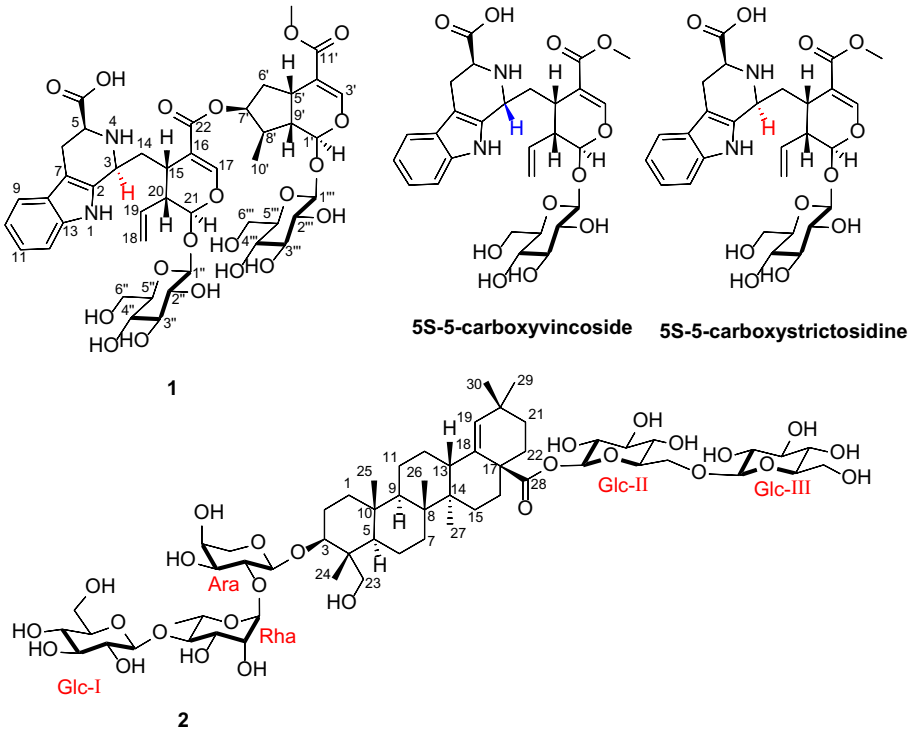

Fig. 1. Structures of compounds **1** and **2**.

(Bruker BioSpin AG, Fällanden, Switzerland) and referenced to solvent peaks (δ_C 49.00 and δ_H 3.31 ppm in CD_3OD). ESIMS analyses were carried out on an Agilent 1260–6460 Triple Quad LC-MS instrument (Agilent Technologies Inc., Waldbronn, Germany). HRESIMS data were acquired on an Agilent 6520 QTOF mass spectrometer (Agilent Technologies Inc., Waldbronn, Germany). All HPLC analyses and separations were performed on Agilent 1260 series LC instruments with 1260 MWD detector (Agilent Technologies Inc., Waldbronn, Germany). All solvents used for column chromatography were of analytical grade (Tianjin Fuyu Fine Chemical Co. Ltd., Tianjin, China) and solvents used for HPLC were of HPLC grade (Oceanpak Alexative Chemical Ltd., Goteborg, Sweden). Agilent SB-C_{18} (9.4 × 250 mm) column (Agilent Technologies Inc., Santa Clara, USA) was used for HPLC separations.

2.2. Plant material

The roots of *Dipsacus asper* Wall. ex C. B. Clarke (Caprifoliaceae) were bought in Kunming 'Juhuayuan' herbal market (collected in September 2016 from An'ning county of Yunnan Province, China) and were authenticated by Prof. Jie Zhou from University of Jinan. A voucher specimen has been deposited at School of Biological Science and Technology, University of Jinan (Accession number: npmc-013).

2.3. Extraction and isolation

The air-dried roots of *Dipsacus asper* (10 kg) were smashed into powder and then extracted with 95% EtOH at room temperature for four times (one week per time). The crude extract (1.0 kg) was partitioned successively with EtOAc/H_2O and *n*-BuOH/H_2O to get EtOAc and *n*-BuOH layers. After evaporation of the solvent of *n*-BuOH partition under reduced pressure, the extract (500 g) was subjected to column chromatography (CC) over D101 macroporous absorption resin, eluted with EtOH-H_2O (0%, 20%, 50%, and 100%, *v*/v) to get four fractions (A, B, C and D). Fraction B (35 g) was subjected to passage over a silica gel column, eluted with $CHCl_3$-MeOH-H_2O (65:15:10, *v*/v), to give four subfractions (B1–B4). Fraction B3 (8.8 g) was then chromatographed on a silica gel CC, eluted with $CHCl_3$-MeOH-EtOAc-H_2O (15:10:40:5, *v*/v), to afford five fractions (B3a–B3e), which were purified in turn by RP-18 CC (10% to 60% MeOH-H_2O, v/v) and semi-preparative HPLC using 45% MeCN-H_2O (v/v, 3.00 mL/min) to obtain **7** (11.6 mg, t_R = 7.0) and **9** (9.1 mg, t_R = 16.2 min), and using 55% MeCN-H_2O (v/v, 3.00 mL/min) to afford compounds **10** (22.3 mg, t_R = 12.5 min), **11** (42.6 mg, t_R = 14.0 min) and **12** (39.3 mg, t_R = 15.2 min). Fraction B4 (4.1 g) was chromatographed on a RP-18 column, eluted with MeOH-H_2O (10% to 60% *v*/v), to obtain two major components, which were further purified by semi-preparative HPLC using 45% MeCN-H_2O (v/v, 3.00 mL/min) as mobile phase to yield compounds **2** (3.0 mg, t_R = 7.5 min) and **14** (12.0 mg, t_R = 8.6 min). Fraction C (52.4 g) was separated by silica gel CC, eluted with $CHCl_3$-MeOH-H_2O (65:15:10, *v*/v), to obtain five fractions (C1–C5). Fraction C2 (10.2 g) was subjected to RP-18 CC, eluted with MeOH-H_2O (20% to 40%, v/v), to give three major fractions (C2a–C2c), each of which was purified by semi-preparative HPLC, using 25% MeCN-H_2O (*v*/v, 3.00 mL/min) as mobile phase, to afford compounds **4** (6.0 mg, t_R = 9.5 min), **16** (9.5 mg, t_R = 11.2 min) and **17** (7.1 mg, t_R = 10.5 min), respectively. Using similar procedures, fraction C4 (15.2 g) was purified by semi-preparative HPLC (3.00 mL/min, 35% MeCN-H_2O, *v*/v) to yield **3** (144.1 mg, t_R = 13.2 min). Fraction C5 (10.5 g) was separated by RP-18 CC, eluted with MeOH-H_2O (20% to 40%, *v*/v), to obtain three fractions (C5a–C5c), which were subsequently purified by semi-preparative HPLC (3 mL/min, 40% MeCN-H_2O, *v*/v) to obtain **1** (19.3 mg, t_R = 12.0 min), **13** (36.4 mg, t_R = 9.7 min) and **5** (27.3 mg, t_R = 8.2 min). Fraction D (45.5 g) was subjected to silica gel CC, eluted with $CHCl_3$-MeOH-H_2O (65:35:10, *v*/v), to afford four fractions (D1–D4). Fraction D3 (28.2 g) was separated firstly using repeated RP-18 CC and further *via* semi-preparative HPLC (3 mL/min, 45% MeCN-H_2O, v/v) to afford compounds **6** (42.8 mg, t_R = 8.8 min), **8** (78.2 mg, t_R = 9.6 min) and **15** (14.2 mg, t_R = 15.3 min).

2.3.1. Dipsaperine (1)

White amorphous powder; $[\alpha]_D^{25}$–137.2 (*c* 1.1, MeOH); UV (MeOH)

Table 1
^{1}H (600 MHz) and ^{13}C (150 MHz) NMR data for **1** in methonal-d_4.

Position	δ_H (*J* in Hz)	δ_C
2		130.3
3	4.54, ddd (12.1, 3.0, 2.5)	53.4
5	3.90, dd (12.1, 4.9)	59.8
6	*α* 3.46, dd (16.2, 4.9)	24.2
	β 3.04, ddd (16.2, 12.1, 2.5)	
7		108.6
8		127.6
9	7.48, d (7.9)	119.4
10	7.05, dd (7.9, 7.0)	120.8
11	7.14, dd (8.2, 7.0)	123.6
12	7.32, d (8.2)	112.4
13		138.7
14	a 2.46, ddd (15.1, 12.5, 3.0)	34.3
	b 2.26, ddd (15.1, 12.1, 3.7)	
15	3.11, m	32.8
16		109.0
17	7.88, br s	157.4
18	a 5.40, br d (17.8)	120.0
	b 5.28, br d (10.6)	
19	5.86, ddd (17.8, 10.6, 7.4)	135.4
20	2.82, m	45.5
21	5.93, d (9.2)	97.7
22		171.3
23		173.7
1′	5.27, d (5.2)	97.8
3′	7.43, br s	152.8
4′		113.2
5′	3.12, m	33.0
6′	*α* 1.77, ddd (14.6, 8.2, 5.0)	40.7
	β 2.36, ddd (14.6, 6.6, 2.4)	
7′	5.30, td (5.0, 2.5)	80.0
8′	2.17, m	41.4
9′	2.09, td (8.7, 5.2)	47.2
10′	1.10, d (6.8)	14.2
11′		169.4
OCH_3	3.69, s	51.9
1″	4.84, d (7.9)	100.7
2″	3.25, dd (9.3, 7.9)	74.8
3″	3.26, dd (9.3, 9.2)	78.1
4″	3.43, dd (9.2, 8.9)	71.9
5″	3.41, ddd (8.9, 7.1, 2.0)	79.0
6″	4.02, dd (11.8, 2.0)	63.2
	3.70, dd (11.8, 7.1)	
1‴	4.65, d (7.9)	100.4
2‴	3.18, dd (9.4, 7.9)	74.9
3‴	3.25, dd (9.4, 9.3)	78.1
4‴	3.37, dd (9.3, 8.9)	71.8
5‴	3.31, ddd (8.9, 6.2, 2.1)	78.5
6‴	3.89, dd (11.9, 2.1)	62.9
	3.63, dd (11.9, 6.2)	

Table 2
^{1}H (600 MHz) and ^{13}C (150 MHz) NMR data for **2** in methonal-d_4.

Position	δ_H (*J* in Hz)	δ_C	Position	δ_H (*J* in Hz)	δ_C
1	*α* 0.94, m	40.1	2	3.64, m	76.8
	β 1.74, m				
2	*α* 1.89, m	26.8	3	3.64, m	74.1
	β 1.77, td (13.3, 3.5)				
3	3.61, dd (12.0, 4.5)	82.4	4	3.76, m	69.8
4		44.1	5	3.84, dd (12.7,3.7)	65.8
				3.51, dd (12.7, 1.8)	
5	1.21, m	48.6	Rha		
6	*α* 1.45, m	18.7	1	5.18, d (2.0)	101.7
	β 1.36, m				
7	1.45, m (2H)	35.2	2	4.24, dd (3.0, 2.0)	71.1
8		41.9	3	3.88, dd (9.5, 3.0)	82.9
9	1.35, m	52.6	4	3.56, dd (9.5, 9.5)	72.6
10		37.9	5	3.92, dq (9.5, 6.1)	70.1
11	*α* 1.59, m	22.2	6	1.25, d (6.1)	18.1
	β 1.33, m				
12	*α* 1.24, m	27.2	Glc-I		
	β 1.58, m				
13	2.28, br d (11.8)	42.3	1	4.50, d (7.8)	105.9
14		43.8	2	3.30, dd (9.2, 7.8)	75.4
15	*α* 1.18, m	30.5	3	3.37, dd (9.2, 8.7)	77.8
	β 1.71, m				
16	*α* 1.44, m	34.6	4	3.33, dd (9.7, 8.7)	71.3
	β 2.22, dt (13.7, 3.3)				
17		49.4	5	3.30, ddd (9.7, 5.1, 1.7)	77.8
18		138.4	6	3.87, dd (12.0, 1.7)	62.4
				3.67, dd (12.0, 5.1)	
19	5.14, s	134.0	Glc-II		
20		33.0	1	5.48, d (8.2)	95.8
21	*α* 1.60, m	34.2	2	3.31, dd (9.3, 8.2)	74.0
	β 2.02, ddd (13.6, 5.8, 3.2)				
22	*α* 1.35, m	34.5	3	3.41, dd (9.3, 8.8)	78.4
	β 1.45, m				
23	0.69, s	13.6	4	3.48, dd (9.7, 8.8)	70.8
24	3.56, d (11.4)	64.5	5	3.52, ddd (9.7, 4.5, 1.9)	78.0
	3.31, d (11.4)				
25	0.93, s	17.9	6	4.13, dd (11.7, 1.9)	69.6
				3.78, dd (11.7, 4.5)	
26	1.02, s	16.8	Glc-III		
27	0.82, s	15.6	1	4.32, d (7.8)	104.9
28		177.0	2	3.21, dd (9.2, 7.8)	75.2
29	0.99, s	29.4	3	3.35, dd (9.2, 8.5)	77.8
30	0.97, s	30.9	4	3.28, dd (9.7, 8.5)	71.6
Ara			5	3.24, ddd (9.7, 5.6, 2.6)	78.0
1	4.49, m	105.1	6	3.86, dd (11.8, 2.6)	62.8
				3.66, dd (11.8, 5.6)	

λ_{max} (log ε) 222 (4.02) nm; ECD (*c* 0.08, MeOH) λ ($\Delta\varepsilon$) 221 (3.10), 236 (−7.07) nm; IR (KBr) ν_{max} 3416, 2924, 2854, 1690, 1630, 1438, 1400, 1076, 744 cm^{-1}; ^{1}H and ^{13}C NMR spectroscopic data (methanol-d_4) see Table 1; (−)-ESIMS: *m/z* 931.7 $[M - H]^-$; (+)-HRESIMS: *m/z* 933.3497 $[M + H]^+$ (calcd for $C_{44}H_{57}N_2O_{20}$, 933.3499).

2.3.2. 3-O-β-D-Glucopyranosyl-(1 → 3)-α-L-rhamnopyranosyl-(1 → 2)-α-L-arabinopyranosyl-23-hydroxyolean-18-en-28-oic acid 28-O-β-D-glucopyranosyl-(1 → 6)-β-D-glucopyranosyl ester (2)

White amorphous powder; $[\alpha]_D^{25}$–30.2 (*c* 0.2, MeOH); IR (KBr) ν_{max} 3402, 2934, 1736, 1639, 1454, 1382, 1070, 630 cm^{-1}; ^{1}H and ^{13}C NMR spectroscopic data (methanol-d_4) see Table 2; (−)-ESIMS: *m/z* 1235.7 $[M - H]^-$, 1271.9 $[M + Cl]^-$; (+)-HRESIMS: *m/z* 1259.6040 $[M + Na]^+$ (calcd for $C_{59}H_{96}O_{27}Na$, 1259.6031).

2.4. ECD calculation of compounds 1a and 1b

The initial conformations of **1a** and **1b** were established *via* the MM2 force field in the ChemDraw_Pro_14.1 software. Conformational searches using mixed torsional/Low-mode sampling method with OPLS3 force field in an energy window of 3.01 kcal/mol were carried out by the conformational search module in the Maestro 10.2 software, returning 48 conformers for **1a** and 47 conformers for **1b**. After eliminating the conformers that did not match the observed coupling constants and NOESY data, 6 and 12 conformers were left for **1a** and **1b**, respectively. The re-optimization and the following TDDFT calculations of the re-optimized conformers were all performed with Gaussian 09 software [7] at the B3LYP/6-311G(d,p) level *in vacuo*. Frequency analysis was performed as well to confirm that the re-optimized conformers were at the energy minima. Finally, the SpecDis 1.64 software [8] was used to obtain the Boltzmann-averaged ECD spectra of **1a** and **1b**.

2.5. Determination of D-glucoses of 1

A solution (1.5 mg) of **1** in 2.0 mol/L HCl (3.0 mL) was stirred at 90 °C for 4 h. After removal of excess HCl under reduced pressure, the residual aqueous mixture was filtered to remove the aglycone part and then evaporated under reduced pressure to afford the free monosaccharides. The obtained monosaccharides were dissolved in ethanol

and then excess (*S*)-(−)-1-phenylethylamine and $NaBH_3CN$ were added. With a catalytic amount of acetic acid added, the mixture was stirred at 40 °C for 3 h. After evaporation of the ethanol, the residue was stirred with acetic anhydride in pyridine at room temperature for 5 h to obtain the amino derivatives. Using the same method, the amino derivatives of authentic L- and D-glucoses were obtained. These derivatives were subjected to HPLC analyses using the following conditions [HPLC column: Agilent ZORBAX SB-C18, 5 μm, 4.6 × 250 mm; Mobile phase: MeCN-H_2O (60%, *v*/v); Flow rate: 1.00 mL/min]. As shown in Fig. S34 [Supplementary material (SM)], the retention times of standard D- and L-glucose derivatives were observed at t_R 5.254 and 4.987 min, respectively, while that of the sugar derivative of **1** was observed at t_R 5.285 min, thus assigning D-configuration for the glucoses in **1**.

2.6. Determination of D-glucoses, L-arabinose and L-rhamnose of 2

Using the same procedure as **1**, the amino derivatives of the hydrolytic sugars from **2** and their corresponding standard ones (D- and L-glucoses, D- and L-arabinoses, and L-rhamnose) were prepared. These derivatives were then subjected to HPLC analyses using the following conditions [HPLC column: Agilent ZORBAX SB-C18, 5 μm, 4.6 × 250 mm; Mobile phase: MeCN-H_2O (50%, *v*/v); Flow rate: 1.00 mL/min]. As shown in Fig. S35 (SM), the retention times for standard D- and L-glucoses, D- and L-arabinoses, and L-rhamnose were at t_R 7.597, 7.219, 6.361, 6.257 and 8.652 min, respectively. The retention times of hydrolytic samples were observed at t_R 7.595, 6.247 and 8.632 min, and thus the D-glucoses, L-arabinose and L-rhamnose were determined for **2**.

2.7. Alkaline hydrolysis

Pure compound **1** (5.0 mg) was digested with 5% NaOH solution (3.0 mL) at 80 °C for 3 h. The reaction mixture was neutralized with 5% HCl solution and then concentrated to dryness. The residue was suspended with ethanol and then filtered to remove NaCl. Compounds **1a** (2.0 mg, t_R = 12.3 min) and **1b** (1.0 mg, t_R = 8.1 min) were finally obtained by HPLC purification using 30% MeCN-H_2O (*v*/v) as mobile phase.

2.7.1. 1a

White amorphous powder; UV (MeOH) λ_{max} (log ε) 221 (3.96) nm; ECD (*c* 0.05, MeOH) λ (Δε) 218 (1.09), 233 (−6.11) nm; (−)-ESIMS: *m/z* 559.3 $[M - H]^-$.

2.7.2. 1b

White amorphous powder; UV (MeOH) λ_{max} (log ε) 232 (3.91) nm; ECD (*c* 0.04, MeOH) λ (Δε) 224 (−2.34), 253 (0.21) nm; (−)-ESIMS: *m/z* 375.1 $[M - H]^-$.

2.8. Cytotoxic assay

The cytotoxic activities of all the compounds were tested using SRB method as we described previously [6]. Adriamycin was used as a positive control.

2.9. AChE inhibitory assay

The AChE inhibitory activities of all the compounds were tested using modified Ellman's method as we described previously [9]. Tacrine was used as a positive control.

3. Results and discussion

Compound **1** was obtained as a white amorphous powder. Its molecular formula of $C_{44}H_{56}N_2O_{20}$ with 18 indices of hydrogen deficiency was deduced from the protonated molecule ion peak at *m/z* 933.3497 $[M + H]^+$ (calcd 933.3499) in (+)-HRESIMS analysis and ^{13}C NMR data. The IR spectrum showed strong absorption bands at 3416, 1690 and 1630 cm^{-1} attributable to hydroxyl, ester carbonyl and olefinic groups, respectively. Two anomeric proton signals at δ_H 4.84 and 4.65 (both d, J = 7.9 Hz), along with the corresponding anomeric carbon signals observed at δ_C 100.7 and 100.4, suggested the presence of two monosaccharide units. Analysis of 1D TOCSY experiments by exciting the aforementioned anomeric protons (Figs. S13 and S14, SM) returned two separate coupling networks, which together with the ^1H–^1H COSY and HSQC data enabled the unambiguous assignments of ^1H and ^{13}C NMR data for the sugar moieties (Table 1). Such information revealed that both monosaccharide units were glucopyranoses [3,10], with β-anomeric configurations being determined by the coupling constants of anomeric protons (both J = 7.9 Hz) [11]. Further HPLC analyses of the (*S*)-(−)-1-phenylethylamine derivatives from the hydrolyzed sugars and authentic D- and L-glucoses (Fig. S34, SM) permitted the assignment of D-configurations for both monosaccharide units. Besides those assignable to the sugar part, the ^1H and ^{13}C NMR data (Table 1) also displayed signals for a carboxyl (δ_C 173.7), two ester carbonyls (δ_C 171.3, 169.4), an ortho disubstituted phenyl (δ_H 7.48, d, J = 7.9 Hz; 7.32, d, J = 8.2 Hz; 7.14, dd, J = 8.2, 7.0 Hz; 7.05, dd, J = 7.9, 7.0 Hz), four double bonds including a monosubstituted terminal one (δ_H 5.40, br d, J = 17.8 Hz; 5.28, br d, J = 10.6 Hz; 5.86, ddd, J = 17.8, 10.6, 7.4 Hz), two trisubstituted ones (δ_H 7.88, 7.43, each br s) and a tetrasubstituted one, two acetal protons (δ_H 5.93, d, J = 9.2 Hz; 5.27, d, J = 5.2 Hz), three oxygenated or ammoniated methines (δ_H 5.30, 4.54, 3.90), and a secondary methyl (δ_H 1.10, d, J = 6.8 Hz). These functionalities and the two glucopyranoses accounted for 13 out of 18

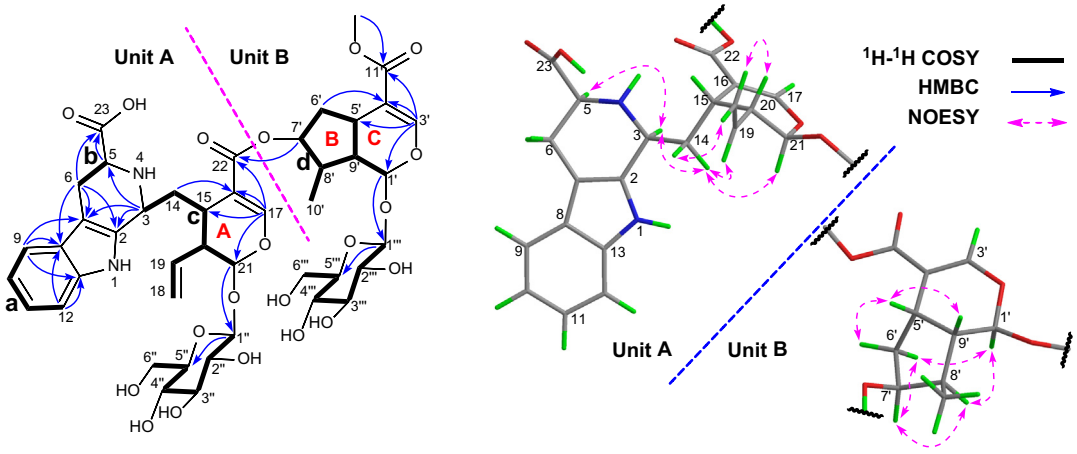

Fig. 2. (A) ^1H–^1H COSY and Key HMBC correlations for **1**; (B) Key NOESY correlations for **1**.

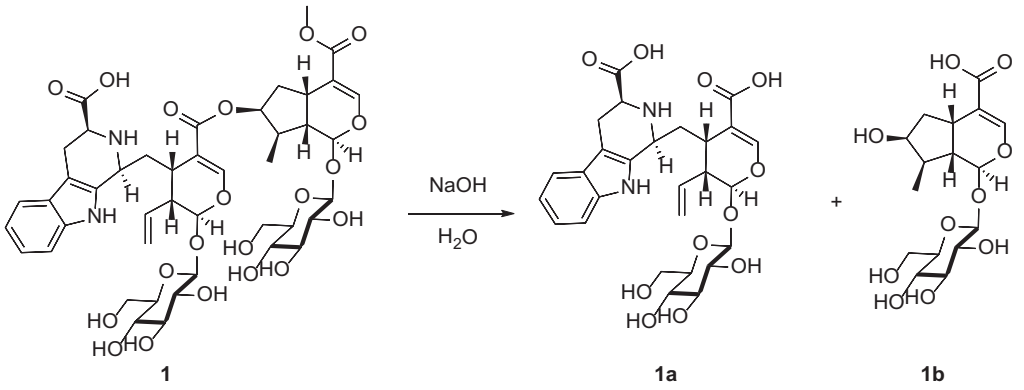

Scheme 1. Alkaline hydrolysis of **1** into **1a** and **1b.**

indices of hydrogen deficiency, thus requiring another five rings in the aglycone part of **1**. Further comprehensive analyses of 2D NMR data (Fig. 2) enabled the assembly of the aforementioned functionalities. In detail, examination of the $^1H-^1H$ COSY data for the aglycone part of **1** (Fig. 2A) furnished four spin-spin coupling systems (**a–d**). The fragments (**a**) and (**b**), together with the HMBC correlations from H-9 to C-7 (δ_C 108.6), C-8 (δ_C 127.6) and C-13 (δ_C 138.7), H_2–6 to C-2 (δ_C 130.3), C-7, C-8 and C-23 (δ_C 173.7), H-3 to C-2, C-5 (δ_C 59.8) and C-7, and H-12 to C-8 and C-13, allowed the construction of a tetrahydro-*β*-carboline-5-carboxylic acid moiety. Afterwards, the fragment (**c**) along with the HMBC correlations from H-17 to C-15 (δ_C 32.8), C-16 (δ_C 109.0), C-21 (δ_C 97.7) and C-22 (171.3), as well as H-21 to C-1″ (δ_C 100.7), assembled another structural motif of a seco-iridoid glucoside and also set up the unit A (Fig. 2A) in **1** as shown. Accordingly, the unit B of an iridoid glucoside residue was established by fragment (**d**) together with the HMBC correlations from H-3′ to C-1′ (δ_C 97.8), C-4′ (δ_C 113.2), C-5′ (δ_C 33.0) and C-11′ (δ_C 169.4), H-1′ to C-1‴ (δ_C 100.4), and OCH_3 to C-11′. Finally, the key HMBC cross-peak from H-7′ to C-22 indicated that units A and B were connected with each other *via* an ester bond. The whole planar structure of **1** was thus elucidated as shown and was the same as that of pterocephaline obtained from *Pterocephalus pinardii* [3]. Comparison of their NMR data revealed that compound **1** differed from pterocephaline mainly in the tetrahydro-*β*-carboline-5-carboxylic acid moiety. Two downfield proton resonances at δ_H 4.54 (ddd, J = 12.1, 3.0, 2.5 Hz, H-3) and 3.90 (dd, J = 12.1, 4.9 Hz, H-5) in **1** were observed, in place of those of δ_H 3.71 (m, H-3) and 3.38 (dd, 13.2, 5.8 Hz, H-5) in pterocephaline, suggesting that the configuration at C-3 in **1** was inverted. However, the structural elucidation of pterocephaline was assigned only by NMR spectroscopic analyses and data comparison without additional evidences [3]. Moreover, compared with those of 5*S*-5-carboxyvincoside (Fig. 1), the H-3 and H-5 resonances in pterocephaline displayed quite obvious differences with each $\Delta\delta_H$ of 0.46 and 0.94 ppm [12], which seemed too large to be convincing. Such inconsistency of NMR data together with the increasing reports of enantiomorphism in nature reminded us that it was not rigorous to perform the structural elucidation of **1** simply *via* NMR data comparison, and the structure of **1** required to be systematically investigated using more strict and credible methods.

Due to the rotational nature of the ester bond linking units A and B, the whole relative configuration of **1** was unable to be directly established, but those of units A and B could be assigned separately by analyzing the NOESY data (Fig. 2B). For unit A, the key strong NOESY correlation between H-21 and H-14a revealed that the CH_2–14 group and H-21 were *quasi*-axially bonded and located at the same side of the half-chair-like A-ring and were randomly assigned an *α*-orientation, thus leaving H-15 *β*-directed. Subsequently, the cross-peaks of H-14a/H-19, H-14b/H-18b and H-18a/H-20 indicated that the terminal double bond was *α*-oriented and located as shown in Fig. 2B. Then the strong correlations of H-14a/H-3 and H-3/H-5, along with the values of $J_{3/14a,b}$ (12.1, 3.0 Hz), assigned the *α*-direction for H-3 and H-5. For unit B, the diagnostic NOESY correlation of H-9′/H-5′ revealed that rings B and C were *cis*-fused, and the two protons were arbitrarily assigned to be *β*-oriented. The relative configurations of other chiral centers were further established as shown on the basis of the strong NOESY correlations of H-5′ with H-6′*β*, H-6′*α* with H-7′ and H-1′, and H-8′ with H-1′and H-7′, which was consistent with loganin (**5**) [13] as also supported by excellent NMR comparisons.

The absolute configuration of **1** was eventually established by separate assignments of its degraded products **1a** and **1b** *via* comparing their respective experimental and calculated ECD data, the latter being acquired by using the time-dependent density functional theory electronic circular dichroism (TDDFT-ECD) method [14]. It should be noted that taking the whole molecule to perform ECD calculation would occupy inestimable computing time due to the reasons listed below: (i) it would generate a great mass of conformations in the conformational search procedure due to the flexibility of the whole molecule; (ii) it would geometrically increase the computing time for each of the conformations in the conformational optimization and ECD calculation procedures due to the large number of atoms; (iii) it would use double computing time due to the unassigned relative configuration of the whole molecule. Fortunately, compound **1** was formed by an indole alkaloid glucoside and an iridoid glucoside *via* an ester bond, so we could selectively cleave the ester bond through alkaline hydrolysis. As described in Scheme 1, compound **1** was hydrolyzed into **1a** and **1b**, and all their ECD spectra were presented in Fig. 3. It was found that the ECD curve of **1a** was much closer than **1b** to that of **1**, demonstrating that unit A had a dominant contribution to the final ECD data of **1**.

The OPLS3 force field with an energy window of 3.01 kcal/mol was used to perform the conformational search of (*3S,5S,15S,16R,21S,1′S,2′R,3′S,4′S,5′R*)-**1a** to obtain 49 conformers. The set of NOEs described in Fig. 2B was employed as a postprocessor

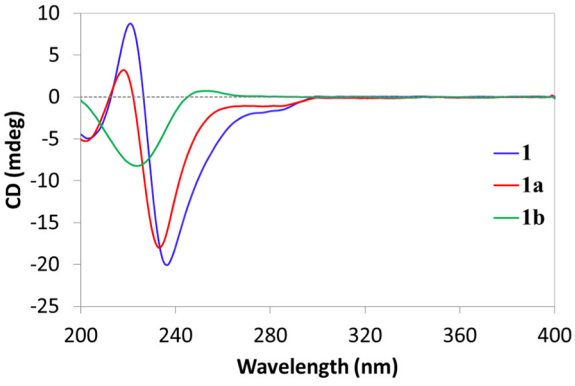

Fig. 3. ECD curves of compounds **1**, **1a** and **1b**.

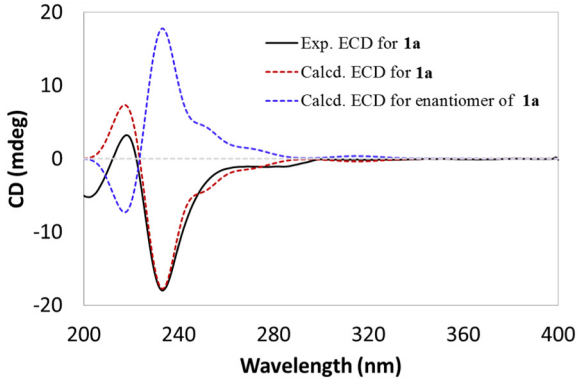

Fig. 4. Experimental ECD spectrum of **1a** (black solid) compared with the calculated ECD spectra of **1a** (red dashed) and its enantiomer (blue dashed). Calculated spectra were plotted as sums of Gaussians with a 0.20 eV exponential half-width. (For interpretation of the references to colour in this figure legend, the reader is referred to the web version of this article.)

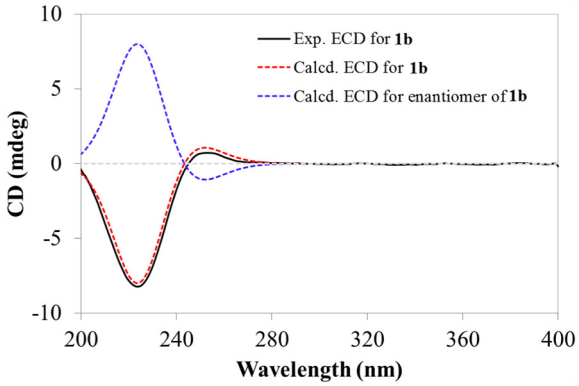

Fig. 5. Experimental ECD spectrum of **1b** (black solid) compared with the calculated ECD spectra of **1b** (red dashed) and its enantiomer (blue dashed). Calculated spectra were plotted as sums of Gaussians with a 0.35 eV exponential half-width. (For interpretation of the references to colour in this figure legend, the reader is referred to the web version of this article.)

filter to eliminate conformers that did not satisfy the observed NOEs. The filtered conformational conformers were then re-optimized with density functional theory (DFT) at the B3LYP/6-311G(d,p) level. Using these DFT-optimized conformers, the quantum-mechanical ECD calculations were carried out with the method of TDDFT at the B3LYP/6-311G(d,p) level. Finally, the Boltzmann-averaged ECD spectrum of **1a** (Fig. 4) furnished a negative Cotton effect at 234 nm and a positive Cotton effect at 219 nm, well matching the experimental ECD spectrum of **1a** (Fig. 4). The absolute configuration of **1a** was then assigned as shown. Using the same force field and energy window as those of **1a**, the conformational search of (*1S,5S,7S,8R,9S,1′S,2′R,3′S,4′S,5′R*)-**1b** gave 47 conformers. After removal of the conformers that did not satisfy the NOEs (Fig. 2B), the remaining 12 conformers were successively re-optimized and ECD calculated using the same methods as those for **1a**. The Boltzmann-averaged ECD spectrum of **1b** was highly consistent with the experimental one (Fig. 5), thus unambiguously assigning the absolute configuration of **1b** as shown. The structure of **1** was thus completely characterized, and this compound was named dipsaperine.

Compound **2** had a molecular formula of $C_{59}H_{96}O_{27}$ as confirmed by the (+)-HRESIMS ion peak at *m/z* 1259.6040 ($[M + Na]^+$, calcd 1259.6031) and the ^{13}C NMR data. The ^1H and ^{13}C NMR spectra showed diagnostic signals for five anomeric protons (δ_H 4.50, 4.49, 4.32, 5.18 and 5.48) and five corresponding carbons (δ_C 105.9, 105.1, 104.9, 101.7 and 95.8), revealing that the structure of **2** contained five monosaccharide units. Further analyses of the 1D-TOCSY (Figs. S29-S33, SM), 2D-HSQC and TOCSY-HSQC (Figs. S22 and S23, SM), and 2D-COSY and HMBC data (Fig. 6A) enabled the assignments of ^1H and ^{13}C NMR data for the aforementioned sugar parts (Table 2). Based on these observations and the HPLC analysis of the sugar derivatives (Fig. S35, SM), the monosaccharides in **2** were finally identified as one *α*-L-arabinopyranose (Ara), one *α*-L-rhamnopyranose (Rha) and three *β*-D-glucopyranoses (Glc) [11,15]. Besides the sugar units, the aglycone moiety featuring a 23-hydroxy-oleanane type triterpenoid skeleton was also uncovered by the NMR data (Table 2), where the diagnostic signals for an ester carbonyl (δ_C 177.0), a trisubstituted double bond (δ_H 5.14, s; δ_C 138.4, 134.0), an oxymethine (δ_H 3.61; δ_C 82.4), an oxygenated methylene (δ_H 3.56, 3.31; δ_C 64.5) and six tertiary methyls (δ_H 1.02, 0.99, 0.97, 0.93, 0.82 and 0.69, each 3H, s), were clearly resolved. The planar structure of **2** was further confirmed by inspection of the HMBC data (Fig. 6A). Particularly, the correlations from H-19 to C-13 (δ_C 42.3), C-17 (δ_C 49.4) and C-18 (δ_C 138.4), and H_3–29/30 to C-19 (δ_C 134.0), located the double bond at Δ^{18}. Furthermore, the HMBC data revealed long-rang correlations between C-3 (δ_C 82.4) of the aglycone and H-1 (δ_H 4.49) of the Ara, as well as between C-2 (δ_C 76.8) of the Ara and H-1 (δ_H 5.18) of the Rha, suggesting the connections of the three structural fragments as shown. In addition, C-4 (δ_C 72.6) of the Rha showed a HMBC correlation with H-1 (δ_H 4.50) of the Glc-I, and thus the construction of a trisaccharide side chain at C-3 of the aglycone moiety was completed. Similarly, a disaccharide side chain was linked to C-28 based on the HMBC correlations from H-1 (δ_H 4.32) of the Glc-III to C-6 (δ_C 69.6) of the Glc-II and H-1 (δ_H 5.48) of the Glc-II to C-28 (δ_C 177.0) of the aglycone.

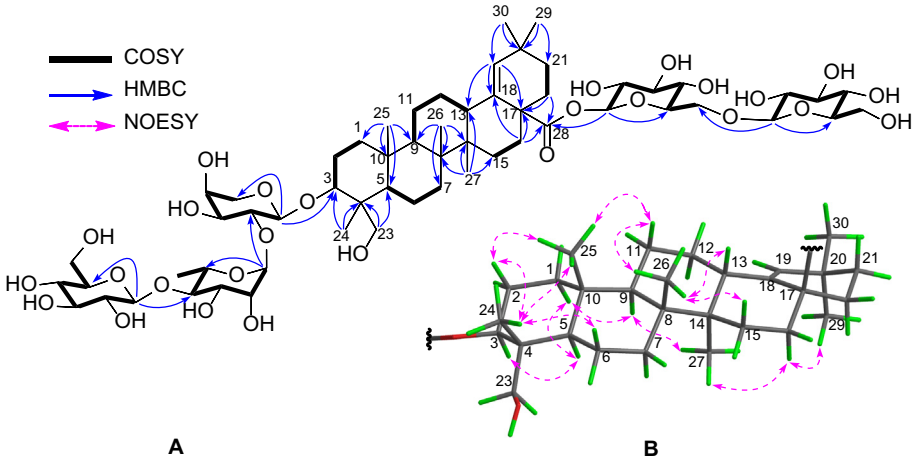

Fig. 6. (A) ^1H–^1H COSY and Key HMBC correlations for **2**; (B) Key NOESY correlations for **2**.

The relative configuration of the aglycone of **2** was established mainly by examination of ROESY data (Fig. 6B). The coupling constants of H-3 with H_2–2 ($J_{2\beta/2\alpha,3}$ = 12.0, 4.5 Hz) revealed that H-3 and H-2β were α- and β-axially directed in the chair-like A-ring, respectively [16,17]. It was followed by the assignment of α-orientation for H-5, H-1α, H-9, H_3-27, H-16α and H_3-29 as deduced from the ROESY correlations of H-3/H-5, H-5/H-1α and H-9, H-9/H_3-27, H_3-27/H-16α and H-16α/H_3-29. In turn, the ROESY cross-peaks of H-2β/H_3-25 and H_3-24, H_3-24/H-6β, H_3-25/H-11β, H-11β/H_3-26, and H_3-26/H-13 and H-15β, allowed these protons to be β-oriented. The structure of **2** was thus characterized as 3-*O*-β-D-glucopyranosyl-(1 → 3)-α-L-rhamnopyranosyl-(1 → 2)-α-L-arabinopyranosyl-23-hydroxyolean-18-en-28-oic acid 28-*O*-β-D-glucopyranosyl-(1 → 6)-β-D-glucopyranosyl ester.

Fifteen known compounds (Fig. S1, SM) were identified to be cocculoside (**3**) [18], swerosid (**4**) [19], loganin (**5**) [13], hederagenin 28-*O*-β-D-glucopyranosyl-(1 → 6)-β-D-glucopyranoside (**6**) [20], 3-*O*-α-L-arabinopyranosylhederagenin 28-*O*-β-D-glucopyranoside (**7**) [21], 3-*O*-α-L-arabinopyranosylhederagenin 28-*O*-β-D-glucopyranosyl(1 → 6)-β-D-glucopyranoside (**8**) [21], 3-*O*-α-L-arabinopyranosyloleanolic acid 28-*O*-β-D-glucopyranosyl-(1 → 6)-β-D-glucopyranoside (**9**) [22], 2′-*O*-acetyl-3-*O*-α-L-arabinopyranosylhederagenin 28-*O*-β-D-glucopyranosyl-(1 → 6)-β-D-glucopyranoside (**10**) [23], 3′-*O*-acetyl-3-*O*-α-L-arabinopyranosylhederagenin 28-*O*-β-D-glucopyranosyl-(1 → 6)-β-D-glucopyranoside (**11**) [24], 4′-*O*-acetyl-3-*O*-α-L-arabinopyranosylhederagenin 28-*O*-β-D-glucopyranosyl-(1 → 6)-β-D-glucopyranoside (**12**) [25], elmalienoside B (**13**) [26], macranthoidin A (**14**) [15], 3-*O*-[β-D-xylopyranosyl-(1 → 4)-β-D-glucopyranosyl-(1 → 4)][α-L-rhamnopyranosyl-(1 → 3)]-β-D-glucopyranosyl-(1 → 3)-α-L-rhamnopyranosyl-(1 → 2)-α-L-arabinopyranosylhederagenin (**15**) [27], 8′-hydroxypinoresinol-4′-*O*-β-D-glucopyranoside (**16**) [28] and 8-hydroxypinoresinol-4′-*O*-β-D-glucopyranoside (**17**) [28] based on spectroscopic analyses and comparison of their NMR data with those reported in the literature.

All of the isolated compounds were tested for their *in vitro* cytotoxicity against four human tumor cell lines of A549 (lung), H157 (lung), HepG2 (liver) and MCF-7 (breast), while only compound **15** displayed significant and also selective inhibition toward the two lung cancer cells with IC_{50} values of 6.94 ± 0.24 (A549) and 9.06 ± 0.12 μM (H157), which was consistent with our previous screening results [6] that the free C-28 carboxyl and 3-*O*-glycosyl groups were necessary for the cytotoxicity of oleanane-type triterpenoid saponins. In addition, the AChE inhibitory activity of **1**–**17** was also evaluated, and only compound **2** showed moderate activity with an IC_{50} value of 15.8 ± 0.56 μM while others were inactive.

4. Conclusions

In summary, an intensive chemical investigation into the *n*-BuOH partition of the ethanol extract from the roots of *D. asper* resulted in the discovery of a rare IMIAH (**1**) featuring a 22-*O*-iridoid glucoside unit, an oleanane triterpenoid saponin (**2**) and 15 known cometabolites. The absolute structure of **1**, a highly complex and flexible molecule, was characterized by a combination of spectroscopic analyses, chemical degradation and quantum chemical computation method. It was the first example that whole absolute configuration was fully established *via* solid evidences among this rare class of natural products with two free iridoid moieties, which provided a beneficial experience for future structure assignments of related analogues. Compounds **2** and **15** were also demonstrated to be mild AChE inhibitor and selective cytotoxic agent, respectively, in the current work.

Conflicts of interest

The authors declare that there is no conflict of interest.

Acknowledgements

This work was funded by Natural Science Foundation of Shandong Province [No. JQ201721 & ZR2018BB023], the Young Taishan Scholars Program [No. tsqn20161037], National Natural Science Foundation of China [No. 21672082], Innovation Team Project of Jinan Science & Technology Bureau [No. 2018GXRC003] and Shandong Talents Team Cultivation Plan of University Preponderant Discipline [No. 10027].

Appendix A. Supplementary data

Supplementary data to this article can be found online at https://doi.org/10.1016/j.fitote.2019.04.015.

References

[1] G.N. Smith, Strictosidine: a key intermediate in the biogenesis of indole alkaloids, Chem. Commun. (15) (1968) 912–914.
[2] W.B. Xin, G.X. Chou, Z.T. Wang, Bis(monoterpenoid) indole alkaloid glucosides from *Uncaria hirsuta*, Phytochem. Lett. 4 (3) (2011) 380–382.
[3] D. Guelcemal, M. Masullo, O. Alankus-Caliskan, T. Karayildirim, S.G. Senol, S. Piacente, E. Bedir, Monoterpenoid glucoindole alkaloids and iridoids from *Pterocephalus pinardii*, Magn. Reson. Chem. 48 (3) (2010) 239–243.
[4] J.H.A. Paul, A.R. Maxwell, W.F. Reynolds, Novel Bis(monoterpenoid) indole alkaloids from *Psychotria bahiensis*, J. Nat. Prod. 66 (6) (2003) 752–754.
[5] A. Itoh, T. Tanahashi, N. Nagakura, T. Nishi, Two chromone-secoiridoid glycosides and three indole alkaloid glycosides from *Neonauclea sessilifolia*, Phytochemistry 62 (3) (2003) 359–369.
[6] J.H. Yu, Z.P. Yu, Y.Y. Wang, J. Bao, K.K. Zhu, T. Yuan, H. Zhang, Triterpenoids and triterpenoid saponins from *Dipsacus asper* and their cytotoxic and antibacterial activities, Phytochemistry 162 (2019) 241–249.
[7] M.J. Frisch, G.W. Trucks, H.B. Schlegel, G.E. Scuseria, M.A. Robb, J.R. Cheeseman, G. Scalmani, V. Barone, B. Mennucci, G.A. Petersson, H. Nakatsuji, M. Caricato, X. Li, H.P. Hratchian, A.F. Izmaylov, J. Bloino, G. Zheng, J.L. Sonnenberg, M. Hada, M. Ehara, K. Toyota, R. Fukuda, J. Hasegawa, M. Ishida, T. Nakajima, Y. Honda, O. Kitao, H. Nakai, T. Vreven, J.A. Montgomery Jr., J.E. Peralta, F. Ogliaro, M. Bearpark, J.J. Heyd, E. Brothers, K.N. Kudin, V.N. Staroverov, R. Kobayashi, J. Normand, K. Raghavachari, A. Rendell, J.C. Burant, S.S. Iyengar, J. Tomasi, M. Cossi, N. Rega, J.M. Millam, M. Klene, J.E. Knox, J.B. Cross, V. Bakken, C. Adamo, J. Jaramillo, R. Gomperts, R.E. Stratmann, O. Yazyev, A.J. Austin, R. Cammi, C. Pomelli, J.W. Ochterski, R.L. Martin, K. Morokuma, V.G. Zakrzewski, G.A. Voth, P. Salvador, J.J. Dannenberg, S. Dapprich, A.D. Daniels, O. Farkas, J.B. Foresman, J.V. Ortiz, J. Cioslowski, D.J. Fox, Gaussian 09 Revision B.01 Gaussian Inc, Wallingford CT (2009).
[8] T. Bruhn, A. Schaumloeffel, Y. Hemberger, G. Bringmann, SpecDis: quantifying the comparison of calculated and experimental electronic circular dichroism spectra, Chirality 25 (4) (2013) 243–249.
[9] Z.Q. Cheng, K.K. Zhu, J. Zhang, J.L. Song, L.A. Muehlmann, C.S. Jiang, C.L. Liu, H. Zhang, Molecular-docking-guided design and synthesis of new IAA-tacrine hybrids as multifunctional AChE/BChE inhibitors, Bioorg. Chem. 83 (2019) 277–288.
[10] F. Li, K. Tanaka, S. Watanabe, Y. Tezuka, I. Saiki, Dipasperoside a, a novel pyridine alkaloid-coupled Iridoid glucoside from the roots of *Dipsacus asper*, Chem. Pharm. Bull. 61 (12) (2013) 1318–1322.
[11] J. Liu, J. Zhang, F. Wang, Y.F. Zou, X.F. Chen, Isolation and characterization of new minor triterpenoid saponins from the buds of *Lonicera macranthoides*, Carbohydr. Res. 370 (2013) 76–81.
[12] N. Aimi, H. Seki, S. Sakai, Synthesis of lyaloside, a prototypal β-carboline gluco indole alkaloid in rubiaceous plants, Chem. Pharm. Bull. 40 (9) (1992) 2588–2590.
[13] S. Lopes, G.L. von Poser, V.A. Kerber, F.M. Farias, E.L. Konrath, P. Moreno, M.E. Sobral, J.A.S. Zuanazzi, A.T. Henriques, Taxonomic significance of alkaloids and iridoid glucosides in the tribe Psychotrieae (Rubiaceae), Biochem. Syst. Ecol. 32 (12) (2004) 1187–1195.
[14] G. Pescitelli, T. Bruhn, Good computational practice in the assignment of absolute configurations by TDDFT calculations of ECD spectra, Chirality 28 (6) (2016) 466–474.
[15] Q. Mao, D. Cao, X.S. Jia, Studies on the chemical constituents of *Lonicera macranthoides* hand. Mazz, Yao Xue Xue Bao 28 (4) (1993) 273–281.
[16] J.H. Yu, Y. Shen, H.B. Liu, Y. Leng, H. Zhang, J.M. Yue, Dammarane-type triterpenoids as 11 beta-HSD1 inhibitors from *Homonoia riparia*, Org. Biomol. Chem. 12 (26) (2014) 4716–4722.
[17] J.H. Yu, Y. Shen, Y. Wu, Y. Leng, H. Zhang, J.M. Yue, Ricinodols A-G: new tetracyclic triterpenoids as 11 beta-HSD1 inhibitors from *Ricinodendron heudelotii*, RSC Adv. 5 (34) (2015) 26777–26784.
[18] F. Sunghwa, M. Koketsu, Phenolic and bis-iridoid glycosides from *Strychnos cocculoides*, Nat. Prod. Res. 23 (15) (2009) 1408–1415.
[19] Y. Zhou, Y.T. Di, S. Gesang, S.L. Peng, L.S. Ding, Secoiridoid glycosides from *Swertia mileensis*, Helv. Chim. Acta 89 (1) (2006) 94–102.
[20] K.Y. Jung, K.H. Son, J.C. Do, Triterpenoids from the roots of *Dipsacus asper*, Arch. Pharm. Res. 16 (1) (1993) 32–35.
[21] S.J. Yang, Z.X. Wu, S.H. Zhou, H.L. Ren, Triterpenoid glycosides from *Dipsacus asperoides* II, J. China Pharm. Univ. 24 (05) (1993) 276–280.

[22] Y.W. Zhang, Z. Xue, Studies on the chemical constituents of *Dipsacus asper* wall, Yao Xue Xue Bao 26 (9) (1991) 676–681.
[23] J.S. Choi, W.S. Woo, Triterpenoid glycosides from the roots of *Patrinia scabiosaefolia*, Planta Med. 53 (1) (1987) 62–65.
[24] Y. Ling, K. Liu, Q. Zhang, L. Liao, Y. Lu, High performance liquid chromatography coupled to electrospray ionization and quadrupole time-of-flight-mass spectrometry as a powerful analytical strategy for systematic analysis and improved characterization of the major bioactive constituents from *Radix Dipsaci*, J. Pharm. Biomed. Anal. 98 (2014) 120–129.
[25] I. Kouno, A. Tsuboi, M. Nanri, N. Kawano, Acylated triterpene glycoside from roots of *Dipsacus asper*, Phytochemistry 29 (1) (1990) 338–339.
[26] N. Sarıkahya, S. Kırmızıgül, Antimicrobially active Hederagenin glycosides from *Cephalaria elmaliensis*, Planta Med. 78 (08) (2012) 828–833.
[27] Y.W. Zhang, Z. Xue, Structure determination of saponin IX and X from *Dipsacus asper* wall, Yao Xue Xue Bao 27 (12) (1992) 912–917.
[28] B. Schumacher, S. Scholle, J. Hoelzl, N. Khudeir, S. Hess, C.E. Mueller, Lignans isolated from valerian: identification and characterization of a new olivil derivative with partial agonistic activity at A1 adenosine receptors, J. Nat. Prod. 65 (10) (2002) 1479–1485.